

Covalent Ag–C Bonding Contacts from Unprotected Terminal Acetylenes for Molecular Junctions

Songsong Li, Hao Yu, Xinyi Chen, Andrew A. Gewirth, Jeffrey S. Moore, and Charles M. Schroeder*



Cite This: <https://dx.doi.org/10.1021/acs.nanolett.0c02015>



Read Online

ACCESS |



Metrics & More



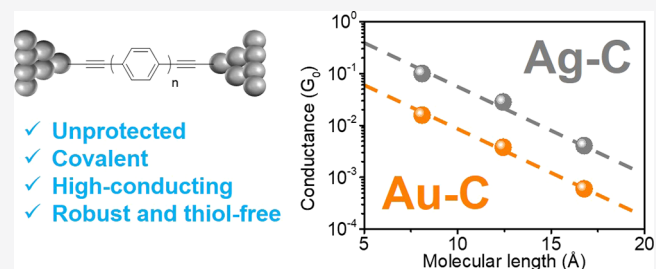
Article Recommendations



Supporting Information

ABSTRACT: Robust molecule–metal linkages are essential for developing high-performance and air-stable devices for molecular and organic electronics. In this work, we report a facile method for forming robust and covalent bonding contacts between unprotected terminal acetylenes and metal (Ag) interfaces. Using this approach, we study the charge transport properties of conjugated oligophenylenes with covalent metal–carbon contacts to silver electrodes formed from unprotected terminal acetylene anchors. We performed single molecule charge transport experiments and molecular simulations on a series of arylacetylenes using gold and silver electrodes. Our results show that molecular junctions on silver electrodes spontaneously form silver–carbynyl carbon (Ag–C) contacts, resulting in a nearly 10-fold increase in conductance compared to the same molecules on gold electrodes. Overall, this work presents a simple, new electrode–anchor pair that reliably forms molecular junctions with stable and robust contacts for molecular electronics.

KEYWORDS: metal–molecule linkages, single molecule conductance, molecular electronics, contact resistance, scanning tunneling microscope break-junction (STM-BJ)



Molecule–electrode interfaces play a key role in controlling the charge transport properties of molecular junctions.¹ Robust, low-resistance contacts between organic molecules and metal electrode interfaces are crucial for building high-performance molecular and organic electronic devices.^{2,3} Linkages between metallic electrodes and organic molecules are commonly achieved using dative anchors (e.g., amine,⁴ methyl sulfide,⁵ pyridine,⁶ and oxazole⁷) or covalent anchors (e.g., thiol⁸) at the termini of molecular junctions. In general, covalent anchors provide ~10 to 100 times lower contact resistance compared to dative anchors, but common covalent anchors suffer from several drawbacks. For example, thiol-based covalent anchors are known to exhibit transient physical adsorption/desorption from metal interfaces, which hinders their use in some practical applications.^{3,8} Moreover, covalent anchors formed from trimethyltin-terminated molecules have shown undesirable dimerization and require the use of toxic reagents,^{9,10} whereas covalent bonds formed based on trimethylsilyl-terminated alkynes require chemical deprotection schemes.^{11,12}

Recently, Olavarria-Contreras et al.¹³ and Bejarano et al.¹⁴ reported the formation of gold–carbon (Au–C) covalent bonds using terminal acetylene anchors without the need for chemical protecting groups. However, this method was not efficient for forming stable junctions involving small molecules (e.g., 1,4-diethynylbenzene). In addition, the conductance of molecular junctions formed by Au–C covalent bonds involving terminal acetylene anchors is approximately 10–100 times

lower than those formed by Au–C covalent bonds from sp^3 carbon.¹³ From this view, there is a need for continued development of robust, reliably formed, and highly conductive covalent linkages for molecule–electrode contacts.

In this work, we report the spontaneous formation of robust and covalent metal–molecule linkages using acetylene-terminated oligophenylenes with silver (Ag) electrodes, resulting in highly conductive molecular wires with significantly lower contact resistance (6 k Ω) compared to those with gold electrodes (36 k Ω). Raman spectroscopy and single molecule conductance experiments provide evidence for the rapid formation of covalent Ag–C bonds, thereby generating stable molecular junctions from acetylene-terminated oligomers and small molecules such as 1,4-diethynylbenzene. Density functional theory (DFT) simulations are further used to elucidate the key role of metal–molecule binding configurations for covalent linkages involving terminal acetylene anchors. Our results also show that conjugated molecules with acetylene anchors exhibit quantum interference effects, such that the molecular conductance ratio (G_{para}/G_{meta})

Received: May 11, 2020

Revised: June 8, 2020

Published: June 8, 2020

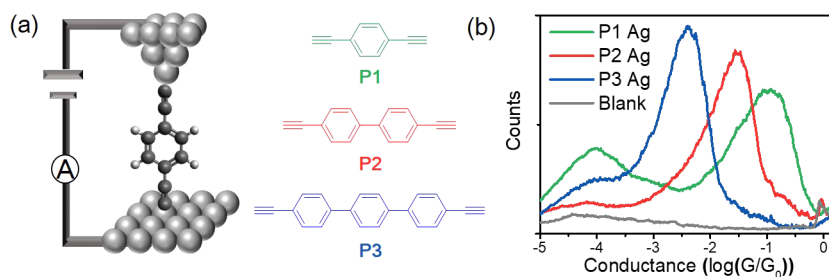


Figure 1. Charge transport in acetylene-terminated molecular wires. (a) Schematic of a Ag–molecule–Ag junction and chemical structures of acetylene-terminated oligophenylene compounds P1–P3. (b) Molecular conductance histograms for P1–P3 using Ag electrodes, each constructed from >4000 single molecule conductance traces.

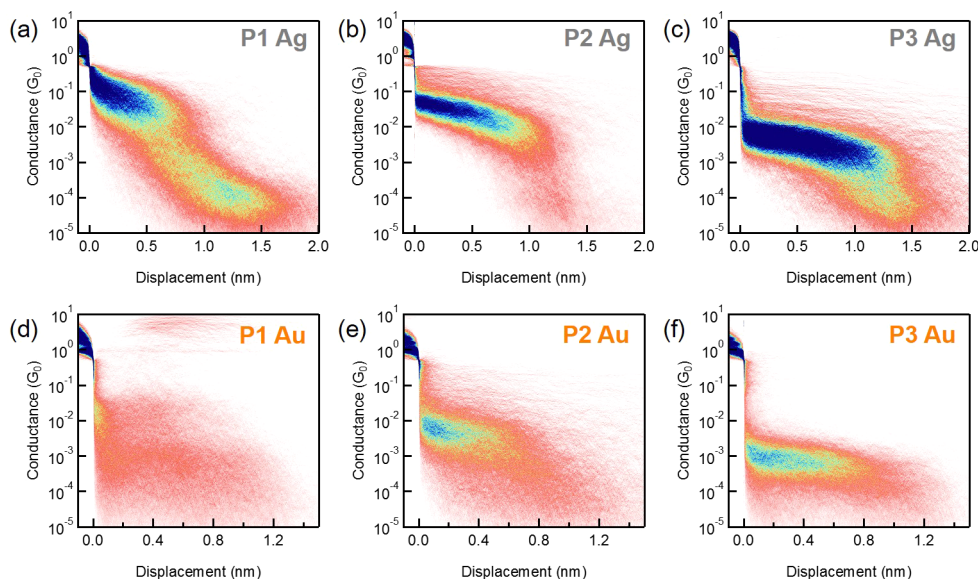


Figure 2. Two-dimensional (2D) molecular conductance histograms for P1–P3 using Ag electrodes (a–c) or Au electrodes (d–f). Each histogram is constructed from >4000 individual traces.

of *para*- versus *meta*-linked diethynylbenzene is significantly larger compared to other commonly used anchors. Taken together, our work provides a straightforward method to achieve robust and thiol-free covalent metal–molecule linkages, thereby opening new avenues for molecular and organic electronics.

We began by characterizing the charge transport properties of a series of acetylene-terminated oligophenylenes (P1–P3) using Ag and Au electrodes. Single molecule conductance is determined using a custom-built scanning tunneling microscope break-junction (STM-BJ) technique under low bias (250 mV) in 1,2,4-trichlorobenzene (1 mM solution) (Figure 1a), as previously described.^{15–17} In particular, single molecule conductance data are collected over the course of 4 h in the STM-BJ instrument following a brief incubation period of a few minutes. Using this approach, one-dimensional (1D) (Figures 1b and S1) and two-dimensional (2D) (Figure 2) molecular conductance histograms are determined for P1–P3, such that each histogram is generated from a large ensemble of >4000 individual molecules. Interestingly, P1 exhibits two peaks in molecular conductance for Ag electrodes, whereas P2 and P3 only show a single prominent peak (Figure 1b). We posit that the lower conductance peak for P1 arises from the spontaneous, *in situ* formation of coordination dimers with silver atoms¹⁸ or from the formation of a diyne by oxidative dimerization¹¹ as previously reported (Figure S2). By fitting

the peaks in the 1D conductance histograms with a Lorentzian function, we determined that the average molecular conductance of P1 is $10^{-1.0} G_0$, while the average conductance values of P2 and P3 are $10^{-1.6} G_0$ and $10^{-2.4} G_0$, respectively ($G_0 = 2e^2/h = 77.5 \mu\text{S}$). Two-dimensional conductance histograms show that the average tip-to-surface displacement at junction breakage increases with molecular length, such that junctions based on P3 are stretched to displacements of ~ 1.5 nm.

To understand the role of metal electrodes on charge transport, we performed single molecule conductance experiments on P1–P3 under the same conditions using gold electrodes (Figures 2d–2f, Figure S1). In contrast to molecular junctions formed with Ag electrodes, we did not observe clear molecular signatures suggestive of stable covalent interactions between P1 and the Au electrodes (Figure 2d), which is consistent with prior work using mechanically controlled break junction (MCBJ) and STM-BJ methods.^{11,13,19} Using Au electrodes, P2 and P3 show appreciable conductance signals, albeit with shorter junction lengths than Ag electrodes (Figure 2e and f). Similar phenomena have been observed in amine- and pyridine-terminated oligophenylenes due to a smaller reorganization time in Ag–molecule–Ag junctions.^{15,20} By analyzing the 1D conductance histograms (Figure S1) with a Lorentzian function, we found that the average molecular conductance values of P2 and P3 with Au electrodes are $10^{-2.4}$

G_0 and $10^{-3.2} G_0$, respectively. Interestingly, the average conductance values of Ag-based junctions for **P2** and **P3** using terminal acetylene anchors are nearly 10× higher compared to junctions formed with Au electrodes.

We next determined the molecular decay constants for acetylene-terminated oligophenylenes with different metal–carbon covalent linkages. Figure 3 shows the average molecular

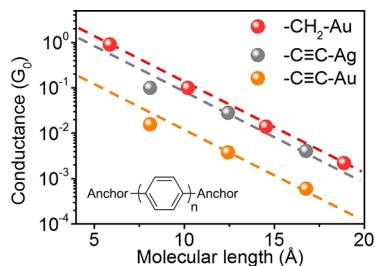


Figure 3. Average molecular conductance of oligophenylenes with different terminal anchors for Au and Ag electrodes. Conductance peak values for $-\text{CH}_2-\text{Au}$ contacts (red, $n = 1, 2, 3, 4$, from ref 9), $-\text{C}\equiv\text{C}-\text{Ag}$ contacts (gray, $n = 1, 2, 3$), and $-\text{C}\equiv\text{C}-\text{Au}$ contacts (orange, $n = 1$ (from ref 11.), 2, 3) are plotted as a function of molecular length. Lines show fits to the data following the equation $G = G_0 e^{-\beta L}$, where β is the molecular conductance decay constant.

conductance plotted on a semilog scale as a function of the distance between distal carbon atoms in terminal anchor groups (determined by DFT calculations). Using a quantum tunneling model such that $G/G_0 = A \exp(-\beta L)$, where A is contact conductance, β is the molecular decay constant, and L is the molecular length between terminal carbon atoms, we determined molecular decay constants $\beta = 0.37 \pm 0.04 \text{ \AA}^{-1}$ (Ag electrodes) and $\beta = 0.38 \pm 0.03 \text{ \AA}^{-1}$ (Au electrodes) for acetylene-terminated oligophenylenes, which is consistent with trimethyltin-terminated ($\beta = 0.43 \text{ \AA}^{-1}$)⁹ and amine-terminated ($\beta = 0.42 \pm 0.01 \text{ \AA}^{-1}$)⁷ oligophenylenes.

We further determined the contact resistance of acetylene-terminated oligophenylene junctions with different metal electrodes. By extrapolating the data in Figure 3 to $L = 0$, we estimated the contact resistance of acetylene–Ag oligophenylene junctions as 6 k Ω , which is significantly smaller than the contact resistance of oligophenylene junctions with acetylene–Au interfaces (36 k Ω), S–Au interfaces (40 k Ω),¹¹ and amine–Au interfaces (189 k Ω).⁷ For these calculations, we used the conductance value of deprotected trimethylsilyl-terminated oligophenylene ethylene (TMS-OPE1) (ref 11) for the contact resistance of deprotonated **P1**. Although CH_2-Au interfaces generally show the lowest contact resistance (1 k Ω), these junctions require the use of toxic reagents and show unavoidable dimerization, which hinders their practical applications.^{9,10} In this way, acetylene-terminated Ag–C junctions readily form robust and highly conductive molecular wires in a straightforward way without the need for complex reaction conditions or chemical protection/deprotection.

We next used surface-enhanced Raman spectroscopy (SERS) to directly probe the formation of covalent Ag–C and Au–C bonds using acetylene-terminated molecules (Figure 4, Figure S3). Self-assembled monolayers are prepared by treating Au or Ag substrates with a solution of 1,2,4-trichlorobenzene containing 1 mM target molecule. Functionalized Au/Ag substrates are then rinsed with acetone and ethanol to remove unbound molecules at various time intervals. Figure 4 shows Raman spectra of **P1–P3** after 24 h incubation time for Au and 4 h for Ag. Three distinct Raman signal regions are shown in Figures 4a and 4b at 1592 cm^{-1} (gray, peak A), 1950–2050 cm^{-1} (blue, peak B), and 2117 cm^{-1} (red, peak C). Peaks A and C are associated with the in-plane stretching mode from the benzene ring and the vibrational stretching mode $\nu(\text{C}\equiv\text{C})_{\text{free}}$ in **P1–P3**, respectively.²¹ Prior work has shown that the $\nu(\text{C}\equiv\text{C})_{\text{free}}$ stretching mode will broaden and shift from 2127 to 2000 cm^{-1} when the *carbynyl*-carbon is covalently bound to metal surfaces.^{11,22–26}

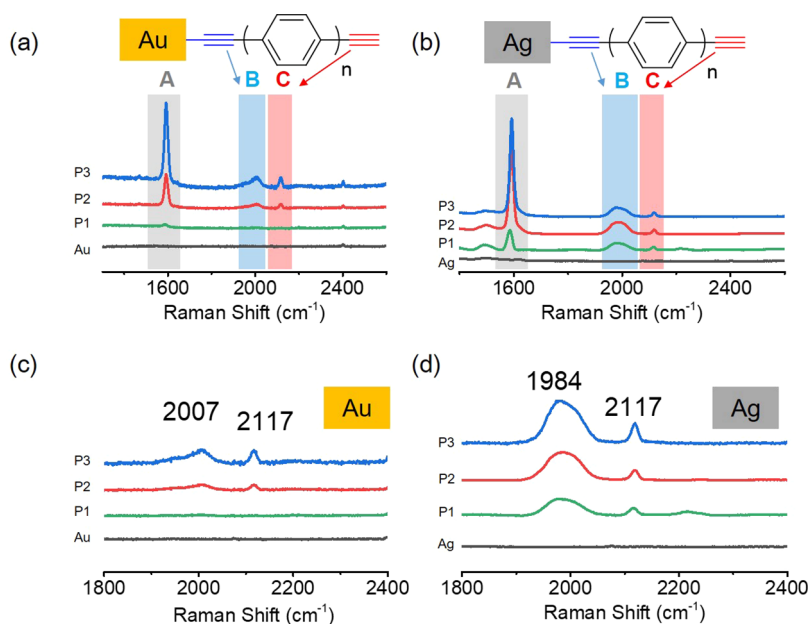


Figure 4. Surface-enhanced Raman spectroscopy (SERS) spectra for **P1–P3** on (a, c) Au substrates and (b, d) Ag substrates. (c, d) Magnified SERS spectra of the relevant $\text{C}\equiv\text{C}$ stretching regions (1800–2400 cm^{-1}) on Au and Ag, respectively.

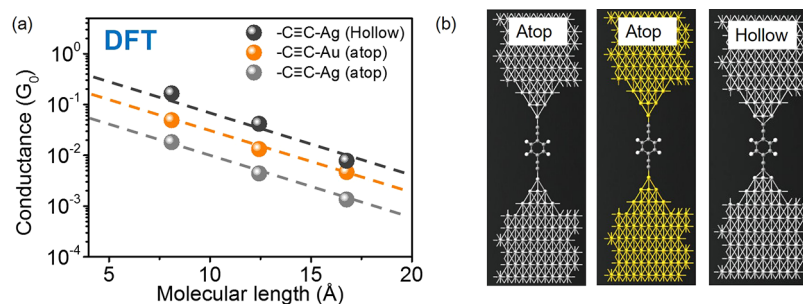


Figure 5. Charge transport behavior of acetylene-terminated oligophenylenes using density functional theory (DFT) simulations. (a) Transmission function values G/G_0 (at $E = E_F$) for acetylene-terminated oligophenylenes with Ag (hollow), Au (atop), and Ag (atop) binding configurations plotted against the molecular length on a semilog scale. (b) Structures of P1 molecular junctions in NEGF-DFT simulations in (a).

Interestingly, a broad peak B around 2000 cm^{-1} $\nu(\text{C}\equiv\text{C})_{\text{bound}}$ was observed on both Au and Ag substrates, which indicates the formation of covalent Au–C and Ag–C bonds.

We further analyzed the relevant regions of Raman spectra, including the $\text{C}\equiv\text{C}$ stretching regions ($1800\text{--}2400\text{ cm}^{-1}$), as shown in Figures 4c and 4d. For P2 and P3, $\nu(\text{C}\equiv\text{C})_{\text{free}}$ and $\nu(\text{C}\equiv\text{C})_{\text{bound}}$ signals were observed on both Au and Ag substrates. In contrast, $\nu(\text{C}\equiv\text{C})_{\text{free}}$ and $\nu(\text{C}\equiv\text{C})_{\text{bound}}$ signals from P1 were only observed on Ag substrates. Strikingly, there is no evidence for P1 binding on Au surfaces even after 24 h incubation time, which agrees with STM-BJ experiments suggesting that P1 does not form stable junctions on Au electrodes (Figure 2d). Interestingly, acetylene-terminated oligophenylene covalently binds to Ag surfaces after incubation after only 5 min at ambient temperature (Figure S4). Taken together, these results directly show that terminal acetylene groups covalently bind to Ag and Au surfaces, with Ag–C linkages forming robust and stable junctions.

Additional evidence for the formation of acetylene–Ag junctions via deprotonation is obtained from single molecule conductance experiments on control molecules, namely, 1,4-bis(phenylethynyl)benzene (P1-Ph), 1,4-dicyanobenzene (P1-CN), and phenylacetylene (H-P1) (Figure S5). Here, we did not observe stable junction formation when the terminal hydrogen is replaced with phenyl (P1-Ph) or nitrogen atoms (P1-CN). Moreover, molecules containing only one terminal acetylene group (H-P1) showed no conductance signal, which suggests that deprotonation on both terminal acetylene groups is necessary to form a stable molecular junction.

To further understand molecular conductance in acetylene-terminated oligophenylenes using Ag and Au electrodes, we used nonequilibrium Green's function-density functional theory (NEGF-DFT) simulations via the Atomistix Toolkit package.^{7,27} Molecular geometries for P1–P3 are optimized with DFT performed on Spartan'16 Parallel Suite using the B3LYP functional with a 6-31G(d,p) basis set. Geometry-optimized molecules are then used to build Au or Ag junctions with different binding configurations, followed by calculation of transmission spectra (Figures S6 and S7).¹² Interestingly, acetylene–Ag contacts with atop binding configurations show smaller transmission values (at $E = E_F$) compared to those with acetylene–Au contacts (Figure 5). However, it is known that acetylene-terminated molecules adopt different binding configurations on metal surfaces, such that binding with atop,²⁸ bridged,²⁹ or hollow²⁹ sites can occur. Therefore, we determined the transmission spectra for Ag junctions with hollow binding configurations (Figure 5). The transmission function values (at $E = E_F$) acetylene–Ag with hollow sites are

larger than those for acetylene–Au with atop sites, which is consistent with the trends in molecular conductance from single molecule experiments. Taken together, these results suggest that different binding motifs of terminal acetylene groups result in a lower Ag–C contact resistance compared to Au–C contacts.

We further examined the role of quantum interference (QI) on molecular junctions formed with terminal acetylene groups.^{30–32} In a single phenyl ring, destructive or constructive QI arises in *meta*- or *para*-linked configurations, respectively, as the de Broglie electron waves emerge either out-of-phase or in-phase after traversing different molecular conduction pathways. In this way, constructive QI generally results in larger values of molecular conductance in *para*-linked phenyl rings.^{33,34} To examine the role of QI in acetylene-terminated phenyl junctions, we studied the molecular conductance of 1,3-diethynylbenzene (P1-*meta*) using Ag electrodes (Figure S8). From the most-probable conductance results, we found that the conductance of P1-*meta* is significantly lower than that of P1, such that $G_{\text{para}}/G_{\text{meta}} = 69$. Surprisingly, these results suggest that acetylene-terminated phenylene shows a larger conductance ratio $G_{\text{para}}/G_{\text{meta}}$ compared to other anchors such as amine ($G_{\text{para}}/G_{\text{meta}} = 2$),³⁵ –SH ($G_{\text{para}}/G_{\text{meta}} = 10$),³⁶ –CH₂SMe ($G_{\text{para}}/G_{\text{meta}} = 2$),³⁷ 4-oxazolyl ($G_{\text{para}}/G_{\text{meta}} = 6.6$),⁷ and 5-oxazolyl ($G_{\text{para}}/G_{\text{meta}} = 6.2$).⁷ In this way, acetylene-terminated phenyl junctions formed with Ag electrodes will facilitate the design of new molecular transistors with large conductance ratios.³⁰

In summary, we used experiments and simulations to show that unprotected acetylene-terminated oligophenylenes form robust and covalent contacts with Ag interfaces. Covalent Ag–C contacts are stable under ambient conditions and spontaneously form without the need for chemical protection/deprotection. Recently, thiol-free metal–molecule linkages have been explored as robust and stable chemistries for organic electronics,³ electrochemistry,³⁸ nanoparticle synthesis,³⁹ and biological investigations.⁴⁰ From this view, our work provides a promising alternative to thiol-based linkers for forming covalent metal–molecule contacts in a straightforward manner. In addition, automated chemical synthesis approaches based on Suzuki coupling are generally compatible with acetylene-terminated molecules, which could enable synthesis of libraries of acetylene-terminated molecules with precise sequence regulation for organic electronics applications.⁴¹ Together, our results open new avenues for building molecular wires with low contact resistance and designing thiol-free metal–molecule linkages for diverse applications.

■ ASSOCIATED CONTENT

SI Supporting Information

The Supporting Information is available free of charge at <https://pubs.acs.org/doi/10.1021/acs.nanolett.0c02015>.

Description of chemical synthesis, chemical and physical characterization of acetylene-terminated molecules, experimental details on STM-BJ, simulation methods, supporting text, and supporting figures (PDF)

■ AUTHOR INFORMATION

Corresponding Author

Charles M. Schroeder – Department of Materials Science and Engineering, Department of Chemical and Biomolecular Engineering, Department of Chemistry, and Beckman Institute for Advanced Science and Technology, University of Illinois at Urbana–Champaign, Urbana, Illinois 61801, United States; orcid.org/0000-0001-6023-2274; Email: cms@illinois.edu

Authors

Songsong Li – Department of Materials Science and Engineering and Beckman Institute for Advanced Science and Technology, University of Illinois at Urbana–Champaign, Urbana, Illinois 61801, United States

Hao Yu – Department of Chemical and Biomolecular Engineering, University of Illinois at Urbana–Champaign, Urbana, Illinois 61801, United States; orcid.org/0000-0002-1594-769X

Xinyi Chen – Department of Chemistry, University of Illinois at Urbana–Champaign, Urbana, Illinois 61801, United States; International Institute for Carbon Neutral Energy Research (WPI-I2CNER), Kyushu University, Fukuoka 819-0385, Japan; orcid.org/0000-0002-6990-5233

Andrew A. Gewirth – Department of Chemistry, University of Illinois at Urbana–Champaign, Urbana, Illinois 61801, United States; International Institute for Carbon Neutral Energy Research (WPI-I2CNER), Kyushu University, Fukuoka 819-0385, Japan; orcid.org/0000-0003-4400-9907

Jeffrey S. Moore – Department of Materials Science and Engineering, Department of Chemical and Biomolecular Engineering, and Beckman Institute for Advanced Science and Technology, University of Illinois at Urbana–Champaign, Urbana, Illinois 61801, United States; orcid.org/0000-0001-5841-6269

Complete contact information is available at: <https://pubs.acs.org/doi/10.1021/acs.nanolett.0c02015>

Notes

The authors declare no competing financial interest.

■ ACKNOWLEDGMENTS

The work was financially supported by the Joint Center for Energy Storage Research (JCESR), an Energy Innovation Hub funded by the U.S. Department of Energy, Office of Science, Basic Energy Sciences, and by the U.S. Department of Defense by a MURI (Multi-University Research Initiative) through the Army Research Office (ARO) through award no. W911NF-16-1-037. X.C. and A.A.G. gratefully acknowledge the support of the International Institute for Carbon Neutral Energy Research (WPI-I2CNER), sponsored by the Japanese Ministry of Education, Culture, Sports, Science, and Technology.

■ REFERENCES

- (1) Su, T. A.; Neupane, M.; Steigerwald, M. L.; Venkataraman, L.; Nuckolls, C. Chemical principles of single-molecule electronics. *Nature Reviews Materials* **2016**, *1*, 16002.
- (2) Xin, N.; Guan, J.; Zhou, C.; Chen, X.; Gu, C.; Li, Y.; Ratner, M. A.; Nitzan, A.; Stoddart, J. F.; Guo, X. Concepts in the design and engineering of single-molecule electronic devices. *Nature Reviews Physics* **2019**, *1*, 211.
- (3) Qiu, X.; Ivasyshyn, V.; Qiu, L.; Enache, M.; Dong, J.; Rousseva, S.; Portale, G.; Stöhr, M.; Hummelen, J. C.; Chiechi, R. C. Thiol-free self-assembled oligoethylene glycols enable robust air-stable molecular electronics. *Nat. Mater.* **2020**, *19*, 330.
- (4) Venkataraman, L.; Klare, J. E.; Nuckolls, C.; Hybertsen, M. S.; Steigerwald, M. L. Dependence of single-molecule junction conductance on molecular conformation. *Nature* **2006**, *442*, 904.
- (5) Li, B.; Yu, H.; Montoto, E. C.; Liu, Y.; Li, S.; Schwieter, K.; Rodríguez-López, J.; Moore, J. S.; Schroeder, C. M. Intrachain Charge Transport through Conjugated Donor-Acceptor Oligomers. *ACS Applied Electronic Materials* **2019**, *1*, 7.
- (6) Kamenetska, M.; Quek, S. Y.; Whalley, A.; Steigerwald, M.; Choi, H.; Louie, S. G.; Nuckolls, C.; Hybertsen, M.; Neaton, J.; Venkataraman, L. Conductance and geometry of pyridine-linked single-molecule junctions. *J. Am. Chem. Soc.* **2010**, *132*, 6817.
- (7) Li, S.; Yu, H.; Schwieter, K.; Chen, K.; Li, B.; Liu, Y.; Moore, J. S.; Schroeder, C. M. Charge Transport and Quantum Interference Effects in Oxazole-Terminated Conjugated Oligomers. *J. Am. Chem. Soc.* **2019**, *141*, 16079.
- (8) Inkpen, M. S.; Liu, Z. F.; Li, H.; Campos, L. M.; Neaton, J. B.; Venkataraman, L. Non-chemisorbed gold-sulfur binding prevails in self-assembled monolayers. *Nat. Chem.* **2019**, *11*, 351.
- (9) Chen, W.; Widawsky, J. R.; Vázquez, H.; Schneebeli, S. T.; Hybertsen, M. S.; Breslow, R.; Venkataraman, L. Highly Conducting π -Conjugated Molecular Junctions Covalently Bonded to Gold Electrodes. *J. Am. Chem. Soc.* **2011**, *133*, 17160.
- (10) Cheng, Z. L.; Skouta, R.; Vázquez, H.; Widawsky, J. R.; Schneebeli, S.; Chen, W.; Hybertsen, M. S.; Breslow, R.; Venkataraman, L. In situ formation of highly conducting covalent Au-C contacts for single-molecule junctions. *Nat. Nanotechnol.* **2011**, *6*, 353.
- (11) Hong, W.; Li, H.; Liu, S.-X.; Fu, Y.; Li, J.; Kaliginedi, V.; Decurtins, S.; Wandlowski, T. Trimethylsilyl-Terminated Oligo-(phenylene ethynylene)s: An Approach to Single-Molecule Junctions with Covalent Au-C σ -Bonds. *J. Am. Chem. Soc.* **2012**, *134*, 19425.
- (12) Tanaka, Y.; Kato, Y.; Tada, T.; Fujii, S.; Kiguchi, M.; Akita, M. Doping of Polyene with an Organometallic Fragment Leads to Highly Conductive Metallapolyene Molecular Wire. *J. Am. Chem. Soc.* **2018**, *140*, 10080.
- (13) Olavarria-Contreras, I. J.; Perrin, M. L.; Chen, Z.; Klyatskaya, S.; Ruben, M.; van der Zant, H. S. J. C-Au Covalently Bonded Molecular Junctions Using Nonprotected Alkynyl Anchoring Groups. *J. Am. Chem. Soc.* **2016**, *138*, 8465.
- (14) Bejarano, F.; Olavarria-Contreras, I. J.; Droghetti, A.; Rungger, I.; Rudnev, A.; Gutiérrez, D.; Mas-Torrent, M.; Veciana, J.; van der Zant, H. S. J.; Rovira, C.; Burzuri, E.; Crivillers, N. Robust Organic Radical Molecular Junctions Using Acetylene Terminated Groups for C-Au Bond Formation. *J. Am. Chem. Soc.* **2018**, *140*, 1691.
- (15) Kim, T.; Vázquez, H.; Hybertsen, M. S.; Venkataraman, L. Conductance of Molecular Junctions Formed with Silver Electrodes. *Nano Lett.* **2013**, *13*, 3358.
- (16) Li, H.; Su, T. A.; Camarasa-Gómez, M.; Hernangómez-Pérez, D.; Henn, S. E.; Pokorný, V.; Caniglia, C. D.; Inkpen, M. S.; Korytár, R.; Steigerwald, M. L.; Nuckolls, C.; Evers, F.; Venkataraman, L. Silver Makes Better Electrical Contacts to Thiol-Terminated Silanes than Gold. *Angew. Chem., Int. Ed.* **2017**, *56*, 14145.
- (17) Yu, H.; Li, S.; Schwieter, K. E.; Liu, Y.; Sun, B.; Moore, J. S.; Schroeder, C. M. Charge Transport in Sequence-Defined Conjugated Oligomers. *J. Am. Chem. Soc.* **2020**, *142*, 4852.
- (18) Vladyka, A.; Perrin, M. L.; Overbeck, J.; Ferradás, R. R.; García-Suárez, V.; Gantenbein, M.; Brunner, J.; Mayor, M.; Ferrer, J. J.

- Calame, M. In-situ formation of one-dimensional coordination polymers in molecular junctions. *Nat. Commun.* **2019**, *10*, 262.
- (19) Pla-Vilanova, P.; Aragonès, A. C.; Ciampi, S.; Sanz, F.; Darwish, N.; Diez-Perez, I. The spontaneous formation of single-molecule junctions via terminal alkynes. *Nanotechnology* **2015**, *26*, 381001.
- (20) Adak, O.; Korytár, R.; Joe, A. Y.; Evers, F.; Venkataraman, L. Impact of Electrode Density of States on Transport through Pyridine-Linked Single Molecule Junctions. *Nano Lett.* **2015**, *15*, 3716.
- (21) Yoo, B. K.; Joo, S.-W. In situ Raman monitoring triazole formation from self-assembled monolayers of 1,4-diethynylbenzene on Ag and Au surfaces via “click” cyclization. *J. Colloid Interface Sci.* **2007**, *311*, 491.
- (22) Fu, Y.; Chen, S.; Kuzume, A.; Rudnev, A.; Huang, C.; Kaliginedi, V.; Baghernejad, M.; Hong, W.; Wandlowski, T.; Decurtins, S.; Liu, S.-X. Exploitation of desilylation chemistry in tailor-made functionalization on diverse surfaces. *Nat. Commun.* **2015**, *6*, 6403.
- (23) Moneo, A.; González-Orive, A.; Bock, S.; Fenero, M.; Herrer, I. L.; Milan, D. C.; Lorenzoni, M.; Nichols, R. J.; Cea, P.; Perez-Murano, F.; Low, P. J.; Martin, S. Towards molecular electronic devices based on ‘all-carbon’ wires. *Nanoscale* **2018**, *10*, 14128.
- (24) Osorio, H. M.; Cea, P.; Ballesteros, L. M.; Gascón, I.; Marqués-González, S.; Nichols, R. J.; Pérez-Murano, F.; Low, P. J.; Martín, S. Preparation of nascent molecular electronic devices from gold nanoparticles and terminal alkyne functionalised monolayer films. *J. Mater. Chem. C* **2014**, *2*, 7348.
- (25) Lissel, F.; Schwarz, F.; Blacque, O.; Riel, H.; Lörtscher, E.; Venkatesan, K.; Berke, H. Organometallic Single-Molecule Electronics: Tuning Electron Transport through X(diphosphine)-2FeC4Fe(diphosphine)2X Building Blocks by Varying the Fe-X-Au Anchoring Scheme from Coordinative to Covalent. *J. Am. Chem. Soc.* **2014**, *136*, 14560.
- (26) Herrer, L.; González-Orive, A.; Marqués-González, S.; Martín, S.; Nichols, R. J.; Serrano, J. L.; Low, P. J.; Cea, P. Electrically transmissive alkyne-anchored monolayers on gold. *Nanoscale* **2019**, *11*, 7976.
- (27) Cai, Z.; Lo, W.-Y.; Zheng, T.; Li, L.; Zhang, N.; Hu, Y.; Yu, L. Exceptional Single-Molecule Transport Properties of Ladder-Type Heteroacene Molecular Wires. *J. Am. Chem. Soc.* **2016**, *138*, 10630.
- (28) Boronat, M.; Combata, D.; Concepción, P.; Corma, A.; García, H.; Juárez, R.; Laursen, S.; de Dios López-Castro, J. Making C-C Bonds with Gold: Identification of Selective Gold Sites for Homo- and Cross-Coupling Reactions between Iodobenzene and Alkynes. *J. Phys. Chem. C* **2012**, *116*, 24855.
- (29) Maity, P.; Takano, S.; Yamazoe, S.; Wakabayashi, T.; Tsukuda, T. Binding Motif of Terminal Alkynes on Gold Clusters. *J. Am. Chem. Soc.* **2013**, *135*, 9450.
- (30) Hsu, L.-Y.; Rabitz, H. Single-Molecule Phenyl-Acetylene-Macrocyclic-Based Optoelectronic Switch Functioning as a Quantum-Interference-Effect Transistor. *Phys. Rev. Lett.* **2012**, *109*, 186801.
- (31) Baghernejad, M.; Zhao, X.; Baruël Ørnsø, K.; Füeg, M.; Moreno-García, P.; Rudnev, A. V.; Kaliginedi, V.; Vesztergom, S.; Huang, C.; Hong, W.; Broekmann, P.; Wandlowski, T.; Thygesen, K. S.; Bryce, M. R. Electrochemical Control of Single-Molecule Conductance by Fermi-Level Tuning and Conjugation Switching. *J. Am. Chem. Soc.* **2014**, *136*, 17922.
- (32) Li, Y.; Buerkle, M.; Li, G.; Rostamian, A.; Wang, H.; Wang, Z.; Bowler, D. R.; Miyazaki, T.; Xiang, L.; Asai, Y.; Zhou, G.; Tao, N. Gate controlling of quantum interference and direct observation of anti-resonances in single molecule charge transport. *Nat. Mater.* **2019**, *18*, 357.
- (33) Gehring, P.; Thijssen, J. M.; van der Zant, H. S. J. Single-molecule quantum-transport phenomena in break junctions. *Nature Reviews Physics* **2019**, *1*, 381.
- (34) Li, X.; Tan, Z.; Huang, X.; Bai, J.; Liu, J.; Hong, W. Experimental investigation of quantum interference in charge transport through molecular architectures. *J. Mater. Chem. C* **2019**, *7*, 12790.
- (35) Kiguchi, M.; Nakamura, H.; Takahashi, Y.; Takahashi, T.; Ohto, T. Effect of Anchoring Group Position on Formation and Conductance of a Single Disubstituted Benzene Molecule Bridging Au Electrodes: Change of Conductive Molecular Orbital and Electron Pathway. *J. Phys. Chem. C* **2010**, *114*, 22254.
- (36) Yang, G.; Wu, H.; Wei, J.; Zheng, J.; Chen, Z.; Liu, J.; Shi, J.; Yang, Y.; Hong, W. Quantum interference effect in the charge transport through single-molecule benzene dithiol junction at room temperature: An experimental investigation. *Chin. Chem. Lett.* **2018**, *29*, 147.
- (37) Borges, A.; Xia, J.; Liu, S. H.; Venkataraman, L.; Solomon, G. C. The Role of Through-Space Interactions in Modulating Constructive and Destructive Interference Effects in Benzene. *Nano Lett.* **2017**, *17*, 4436.
- (38) Crudden, C. M.; Horton, J. H.; Ebralidze, I. I.; Zenkina, O. V.; McLean, A. B.; Drevniok, B.; She, Z.; Kraatz, H.-B.; Mosey, N. J.; Seki, T.; Keske, E. C.; Leake, J. D.; Rousina-Webb, A.; Wu, G. Ultra stable self-assembled monolayers of N-heterocyclic carbenes on gold. *Nat. Chem.* **2014**, *6*, 409.
- (39) Narouz, M. R.; Osten, K. M.; Unsworth, P. J.; Man, R. W. Y.; Salorinne, K.; Takano, S.; Tomihara, R.; Kaappa, S.; Malola, S.; Dinh, C.-T.; Padmos, J. D.; Ayoo, K.; Garrett, P. J.; Nambo, M.; Horton, J. H.; Sargent, E. H.; Häkkinen, H.; Tsukuda, T.; Crudden, C. M. N-heterocyclic carbene-functionalized magic-number gold nanoclusters. *Nat. Chem.* **2019**, *11*, 419.
- (40) MacLeod, M. J.; Goodman, A. J.; Ye, H.-Z.; Nguyen, H. V. T.; Van Voorhis, T.; Johnson, J. A. Robust gold nanorods stabilized by bidentate N-heterocyclic-carbene-thiolate ligands. *Nat. Chem.* **2019**, *11*, 57.
- (41) Li, J.; Ballmer, S. G.; Gillis, E. P.; Fujii, S.; Schmidt, M. J.; Palazzolo, A. M. E.; Lehmann, J. W.; Morehouse, G. F.; Burke, M. D. Synthesis of many different types of organic small molecules using one automated process. *Science* **2015**, *347*, 1221.